*Dynamical evolution of dense stellar systems*
*Proceedings IAU Symposium No. 246, 2007*
*E. Vesperini*


DOI: 00.0000/X000000000000000X

# Observational evidence for the origin of X-ray sources in globular clusters

**Frank Verbunt[1], Dave Pooley[2] and Cees Bassa[3]**

[1]Astronomical Institute, Postbox 80.000, 3508 TA Utrecht, the Netherlands
email: verbunt@astro.uu.nl

[2]Dept. of Astronomy, University of Wisconsin-Madison Madison WI 53706-1582, U.S.A.
email: dave@astro.wisc.edu

[3]Physics Department, McGill University, Montreal, QC H3A 2T8 Canada
email: bassa@physics.mcgill.ca



**Abstract.** Low-mass X-ray binaries, recycled pulsars, cataclysmic variables and magnetically active binaries are observed as X-ray sources in globular clusters. We discuss the classification of these systems, and find that some presumed active binaries are brighter than expected. We discuss a new statistical method to determine from observations how the formation of X-ray sources depends on the number of stellar encounters and/or on the cluster mass. We show that cluster mass is not a proxy for the encounter number, and that optical identifications are essential in proving the presence of primordial binaries among the low-luminosity X-ray sources.

**Keywords.** X-ray sources, globular clusters, stellar encounters

## 1. Introduction

The first celestial maps in X-rays, in the early 1970s, show that globular clusters harbour more X-ray sources than one would expect from their mass. As a solution to this puzzle it was suggested that these bright ($L_x \gtrsim 10^{36}$ erg/s) X-ray sources, binaries in which a neutron star captures mass from a companion star, are formed in close stellar encounters. A neutron star can be caught by a companion in a tidal capture, or it can take the place of a star in a pre-existing binary in an exchange encounter. Verbunt & Hut (1987) showed that the probability of a cluster to harbour a bright X-ray source indeed scales with the number of stellar encounters occurring in it; whereas a scaling with mass does not explain the observations.

With the *Einstein* satellite a dozen less luminous ($L_x \lesssim 10^{35}$ erg/s) X-ray sources were discovered in the early 1980. *ROSAT* enlarged this number to some 55, and now thanks to *Chandra* we know hundreds of dim X-ray sources in globular clusters. The nature and origin of these dim sources is varied. Those containing neutron stars, i.e. the quiescent low-mass X-ray binaries in which a neutron star accretes mass from its companion at a low rate and the recycled or millisecond radio pulsars, have all formed in processes involving close stellar encounters. The magnetically active binaries, on the other hand, are most likely primordial binaries, with stars that are kept in rapid rotation via tidal interaction. Cataclysmic variables are binaries in which a white dwarf accretes matter from a companion. In globular clusters they may arise either via stellar encounters, or from primordial binaries through ordinary binary evolution – this is expected to depend on the mass and density of the globular cluster.

In this paper we describe the classification and identification of the dim sources in Section 2, and make some remarks on the theory of their formation in Section 3. In Section 4

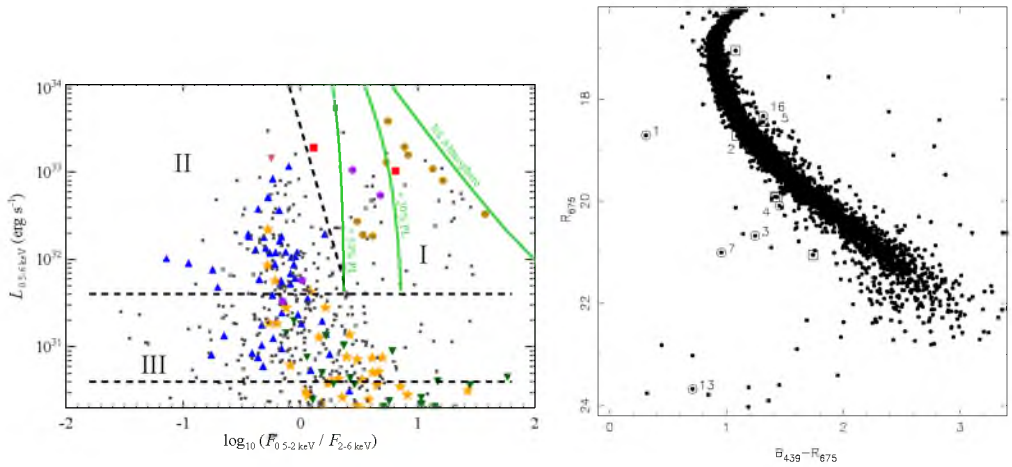


**Figure 1.** Left: X-ray hardness-luminosity diagram for dim sources in globular clusters. I: quiescent low-mass X-ray binaries, II: cataclysmic variables III: cataclysmic variables and magnetically active binaries. From Pooley & Hut (2006). Right: Colour-magnitude diagram of NGC 6752 on the basis of HST-WFPC2 data; objects within X-ray position error circles are marked. Left of the main sequence we find cataclysmic variables, above it active binaries. Updated from Pooley et al. (2002a).

we will discuss a new, and in our view more accurate, way to compare the numbers of these sources with theoretical predictions.

## 2. Clasification and identification

Work on the dim sources is progressing along various lines. Grindlay and coworkers study one cluster, 47 Tuc, in great detail (Grindlay et al. 2001, Edmonds et al. 2003, Heinke et al. 2005). Webb and coworkers use XMM to obtain high-quality X-ray spectra (e.g. Webb et al. 2006, Servillat this meeting). Dim sources are also found in clusters in which individual sources are the main target, such as Terzan 1 and 5, and M 28 (Wijnands et al. 2002, Heinke et al. 2003, Becker et al. 2003). Lewin initiated a large program to observe clusters with very different central densities and core radii, and thereby to provide material for tests on the dependence on these properties of the numbers of dim sources. Further references to all this work may be found in the review by Verbunt & Lewin (2006); and in the remainder of this Section.

The first classification of the dim sources may be made on the basis of the **X-ray properties only** (Fig. 1). The brightest sources in the 0.5-2.5 keV band, at $L_x \gtrsim 10^{32}$ erg/s, tend to be quiescent low-mass X-ray binaries. To better use the Chandra range, one may also select the brightest sources in the 0.5-6.0 keV band, and select soft sources, with a high ratio of fluxes below and above e.g. 2 keV: $f_{0.5-2.0\mathrm{keV}}/f_{2.0-6.0\mathrm{keV}} \gtrsim 1$. Such sources also are mostly quiescent low-mass X-ray binaries. Between $10^{31}$ and $10^{32}$ erg/s most sources are cataclysmic variables, especially when they have hard spectra $f_{0.5-2.0\mathrm{keV}}/f_{2.0-6.0\mathrm{keV}} < 1$. The faintest sources include magnetically active binaries, often with soft X-ray spectra. For many faint sources the number of counts is too low to decide on the hardness of the spectrum.

The second step in classification can be made when **identification** with a source **at other wavelengths** is made. Positional coincidence of an X-ray source with the accurate radio position of a millisecond pulsar provides a reliable identification and classification. Positional coincidence with optical sources is only significant if the highest possible as-

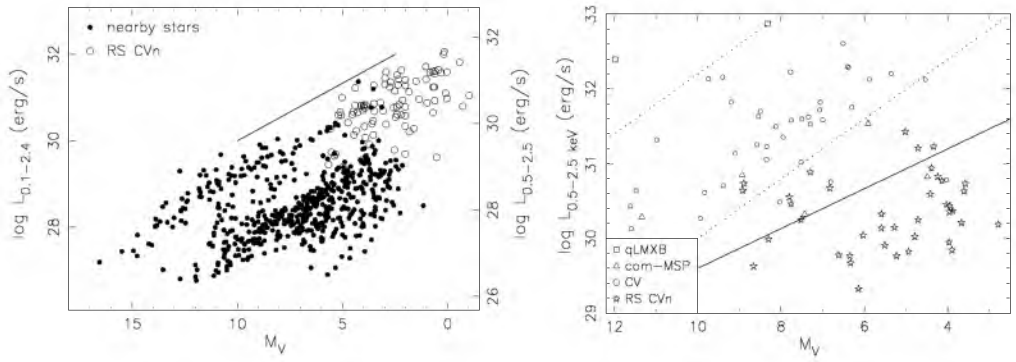


**Figure 2.** Left: X-ray luminosity as a function of absolute visual magnitude for nearby stars (*selected* from Hünsch et al. 1999, for details see Verbunt 2001) and for RS CVn systems (from Dempsey et al. 1993). The upper bound Eq. 2.3 is indicated with a solid line. We convert the X-ray fluxes in the 0.1-2.4 keV range (scale on the left) to the 0.5-2.5 keV range by multiplication with 0.4 (scale on the right). Right: X-ray luminosity as a function of absolute visual magnitude, for dim X-ray sources in globular clusters. The assumed separatrices Eqs. 2.1,2.2 are indicated with dotted lines, the upper bound Eq. 2.3 with a solid line. It is seen that some X-ray sources classified as active binaries in globular clusters are well above this bound.

trometric accuracy is used to limit the number of possible counterparts (e.g. Bassa et al. 2004). The position of these possible counterparts in a colour-magnitude diagram is then used to select the probable counterparts. Cataclysmic variables are bluer than the main sequence stars, and magnetically active binaries may lie above the main sequence. Systems on the main sequence cannot be unambiguously classified: they may either be cataclysmic variables in which the optical flux is dominated by the donor star, or main-sequence binaries with unequal masses whose optical light is dominated by the brighter star. If a periodicity is found in the X-rays that corresponds to a period at another wavelength, e.g. the pulse period of a pulsar or the orbital period of a binary, identification and clasification are secured simultaneously (e.g. Ferraro et al. 2001).

A very useful discriminant in X-ray astronomy in general is the X-ray to optical flux ratio. In the case of globular clusters we can use the known distance to determine the **optical to X-ray luminosity ratio** (Fig 2). On the basis of in particular the extensive data on 47 Tuc (Edmonds et al. 2003 and references therein) one finds that the lines of constant optical to X-ray luminosity ratio

$$\log L_{0.5-2.5\mathrm{keV}}(\,\mathrm{erg/s}) = 36.2 - 0.4 M_\mathrm{V} \tag{2.1}$$

separates the quiescent low-mass X-ray binaries above it from the cataclysmic variables below. The line

$$\log L_{0.5-2.5\mathrm{keV}}(\,\mathrm{erg/s}) = 34.0 - 0.4 M_\mathrm{V} \tag{2.2}$$

roughly separates the cataclysmic variables from the magnetically active binaries.

This latter separatrix leads to a surprise when one compares it with the X-ray luminosities of nearby stars and of known magnetically active binaries, i.e. RS CVn systems, near the Sun. For main-sequence stars in the solar neighbourhood, the X-ray luminosity increases with the rotation speed, up to an upper bound given approximately by

$$\log L_{0.5-2.5\mathrm{keV}}(\,\mathrm{erg/s}) = 32.3 - 0.27 M_\mathrm{V} \tag{2.3}$$

as illustrated in Fig. 2 (left). This bound is lower than the separatrix given by Eq. 2.2, especially for brighter stars. This would imply that active binaries in globular clusters can have higher X-ray luminosities than similar binaries near the Sun. We suggest, how-

ever, that the classification must be reinvestigated, and that some of these objects are cataclysmic variables. The absence of the blue colour expected for a cataclysmic variable (see Fig. 1) then requires explanation – e.g. as a consequence of the non-simultaneous measurements at different colours combined with source variability.†

## 3. Some remarks on theory

Binaries in a globular clusters change due to their internal evolution and/or due to external encounters. To describe the current cluster binary population one must track the events for each primordial binary and for each binary that is newly formed via tidal capture, throughout the cluster. The first estimates of the formation of binaries with a neutron star necessarily made a number of drastic simplifications. The sum of all encounters (of a neutron star with a single star, or with a binary) was replaced with an integral over the cluster volume of the encounter rate per unit volume. Four assumptions followed: the number density $n_1, n_2$ of each participant in the encounter scales with the total mass density $\rho$, the relative velocity between the encounter participants scales with the velocity dispersion $v$, the interaction cross section $A$ is dominated by gravitational focussing so that $A \propto 1/v^2$, and the encounter rate is dominated by the encounters in the dense cluster core. Hence one writes the cluster encounter rate $\Gamma'$ as

$$\Gamma' = \int_V n_1 n_2 A v dV \propto {\rho_o}^2 {r_c}^3 / v \tag{3.1}$$

where $\rho_o$ is the central density and $r_c$ the core radius. If one further eliminates the velocity dispersion through the virial theorem, $v \propto r_c \sqrt{\rho_o}$, one has

$$\Gamma' \propto {\rho_o}^{1.5} {r_c}^2 \equiv \Gamma \tag{3.2}$$

where $\Gamma$ is referred to as the collision number. With a life time $\tau$ the expected number of binaries of a given type is

$$N = \Gamma' \tau \propto \Gamma \tau \tag{3.3}$$

A major advantage of these simple estimates is the clear connection between (the uncertainty in) the input and (the uncertainty of) the output. Thus, if $n_1, n_2$ are the number densities of neutron stars and of binaries, respectively, Eqs. 3.1-3.3 indicate that the uncertainty in the number $N$ of neutron star binaries scales directly with the uncertainties in $n_1$ and $n_2$. Similarly, if we overestimate the life time $\tau$ of a binary by a factor 10, the estimated number $N$ is overestimated by the same factor.

Thanks to a concerted effort by various groups fairly detailed computations of the happenings in globular clusters are now undertaken. This is a fortunate and necessary development, as many details cannot be understood from the simple scalings above. For example, the wide progenitors of cataclysmic variables are destroyed by close encounters before they evolve in a dense cluster core (Davies 1997), but evolve undisturbed into cataclysmic variables in the outer cluster regions, from where they can sink to the dense core to form a significant part of the current population there (Ivanova et al. 2006).

A disadvantage of complex computations is that they tend to hide the uncertainties. If the cross sections $A$ are described in paper I of a series, and the life times $\tau$ in paper III, the large uncertainties in them tend to be less than obvious in paper V where the

† In his contribution to this meeting, Christian Knigge shows that the tentative counterpart of W24 in 47 Tuc, a possible active binary according to Edmonds et al. (2003, Sect.4.5), has blue FUV-U colours, which suggests that it is a cataclysmic variable. At $M_V = 2.6$ and $L_x = 8.7{\times}10^{30}$ erg/s, it actually lies below the line given by Eq. 2.3.

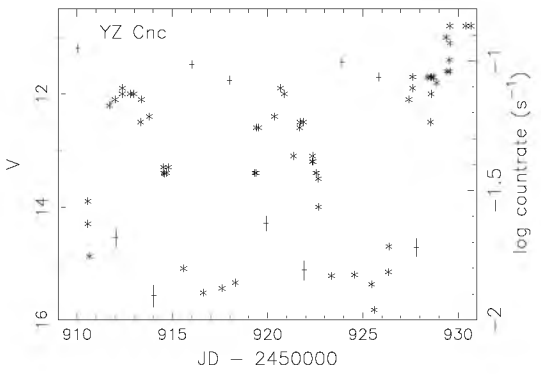


**Figure 3.** Optical (*, scale on left) and X-ray (+, scale on right) lightcurves of the dwarf nova YZ Cnc through several outburst cycles: the outburst in the optical luminosity is accompanied by a marked *drop* in the X-ray luminosity. After Verbunt et al. (1999)

final computations are described. The confidence expressed in summaries of the results of such computations is sometimes rather larger than warranted. An uncertainty in $A$ or $\tau$ has an equally large effect in complex computations as in simple estimates. As a further illustration we discuss two other uncertainties.

The first relates to the question what happens when mass transfer from a giant to its binary companion is dynamically unstable. It is usually assumed that a spiral-in follows, in which the companion enters the envelope of the giant and expells it through friction. The outcome of this process is computed using conservation of energy, which implies a drastic shrinking of the orbit (Webbink 1984). However, the study of nearby binaries consisting of two white dwarfs shows that the mass ratios in them are close to unity (e.g. Maxted et al. 2002). Such binaries can only be explained if the consequences of dynamically unstable mass transfer are governed by conservation of angular momentum, rather than by the energy equation. If the mass leaving the binary has roughly the same specific angular momentum as the binary, the orbital period changes relatively little during the unstable mass transfer and concomitant mass loss from the binary (Van der Sluys et al. 2006). The standard prescription of dynamically unstable mass transfer hitherto implemented in globular cluster computations must be replaced.

The second uncertainty relates to the conversion of the mass transfer rate in a cataclysmic variable to the X-ray luminosity. This conversion does not affect the evolution of the binary but it is important for comparison with observations, as most cataclysmic variables in globular clusters are discovered as X-ray sources. It is generally assumed that the X-ray luminosity scales directly with the mass transfer rate: $L_x \propto \dot{M}$. Alas, reality is more complicated, and indeed in most cases the X-ray luminosity goes down when the mass transfer rate goes up. This is demonstrated unequivocally in dwarf novae whose X-ray luminosity drops precipitously during outbursts (Fig. 3), but there is evidence that it is true in the more stable nova-like variables as well (Verbunt et al. 1997). But exceptions are also known: the dwarf nova SS Cyg has higher X-ray flux during outburst than in quiescence (Ponman et al. 1995). Theoretical predictions of the numbers of cataclysmic variables in globular clusters that radiate detectable X-ray fluxes, are not believable when based on proportionality of X-ray flux and mass-transfer rate.

Observational evidence for the numbers of binaries of various types, and of the dependence of these numbers on cluster properties, may be collected and used to constrain the theories on formation and evolution of various types of binaries in globular clusters (e.g. Pooley et al. 2003, Heinke et al. 2006, Pooley & Hut 2006).

In the next Section we describe a new, and we hope more accurate, method of analysing source numbers: this method is based on direct application of Poisson statistics. This topic brings one of us, FV, to a brief Intermezzo.

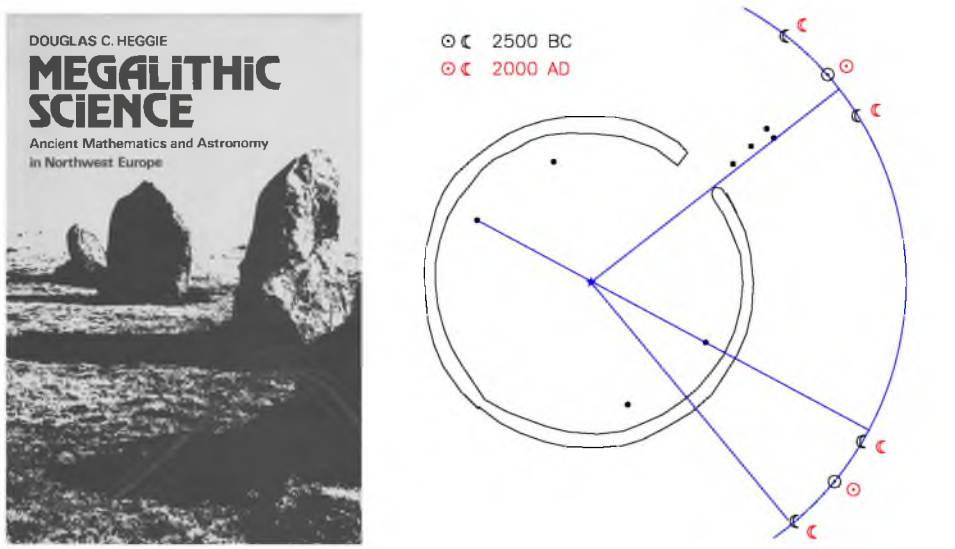


**Figure 4.** Left: the classic book by Douglas Heggie on Megalithic Science. Right: Sketch of Stonehenge with the circular bank & ditch (the *henge*), the rectangle of the four Station Stones within it, and the directions towards the extreme risings of Sun and Moon at the winter and summer solstitia of 2500 B.C. and 2000 A.D. The minute shift in 4500 yr is due to the small change in obliquity.

## Intermezzo by FV: another side of Douglas Heggie

The first time that I had need of understanding of binomial and Poisson statistics was in the early 1980s, when I bought a book by Douglas Heggie (1981) called *Megalithic Science, Ancient Mathemathics and Astronomy in Northwest Europe*. The first half of this book discusses the question whether the megalith builders used a standard measure of length (the answer is no), and the second half studies the question whether megalithic structures had astronomical orientations. Whereas Douglas is still rather modest about this book, it is still *the best introduction to the issues in megalithic astronomy* (McCluskey 1998, p.11). It, for the first time, explained the statistics of the study of astronomical orientations of megalithic structures. In my view it is not an exaggeration to state that archaeo-astronomy may be divided in a pre-Heggie era, in which the statistics is usually wrong, and a post-Heggie era, in which at least some people, following Douglas's prescription, do their statistics right. Among the latter I may specifically mention Ruggles (1999).

As an example of an application of binomial statistics I paraphrase the discussion on p.198 of the book, of the four Station Stones in Stonehenge. These Stones were placed, near 2500 B.C., in a rectangle with the short sides parallel to the main axis of Stonehenge (Fig. 4). This main axis points from the center of the rectangle through a gap in the bank-plus-ditch (the *henge*) surrounding it toward the location on the horizon of the most northern annual rising of the Sun, at summer solstice. The Moon ranges in a 19 yr cycle from about 5° north of the Sun to 5° south of the Sun, which leads to a range of its most northern and southern annual risings. The extremes of these ranges, together with the two solstitia, define 6 positions on the eastern horizon. Accepting a range of $\pm 1.8°$ for each position, we find a probability that an arbitrary direction towards the eastern horizon hits one of these positions $p = 6 \times 2 \times 1.8/180 = 0.12$. The rectangle of the Station Stones defines three new directions towards the East: along the long side and along the diagnonals. Two of these hit one of the 6 positions: extremes of the southernmost annual setting of the Moon in the 19 yr cycle. The probability of 1 chance hit in 3 trials with

$p = 0.12$ is 28%, the probability of 2 chance hits 4%. Most likely one hit is due to chance, and one hit intentional.

Thanks to new research at Stonehenge, done after the publication of *Megalithic Science*, we now know that the central structure, circle and horse-shoe form, were put up simultaneous with the Station Stones, which implies that the view along the diagonals was blocked. The intentional hit is therefore the one along the long side. Since the long side of a rectangle is necessarily perpendicular to the short side, this implies that the location of Stonehenge was selected for its latitude.

## 4. Testing models against observations

For the denser clusters it is found that the X-ray sources lie well within the half-mass radius (e.g. NGC 6440, Fig.1 of Pooley et al. 2002b), whereas for (apparently) large clusters only the area within the half-mass radius is covered (e.g. 47 Tuc, Grindlay et al. 2001). Thus, the analysis generally deals with the sources within the half-mass radius. If $N_h$ is the observed number of X-ray sources, and $N_b$ the number of background (or foreground) sources not related to the cluster, the number of cluster sources within the half-mass radius is $N_c = N_h - N_b$. From a model we may obtain an estimate of the expected number of cluster sources $\mu_c$, and we also may estimate the expected number of background sources $\mu_b$.

In clusters with a small number of sources, $N_c \lesssim 10$, say, one cannot apply chi-squared statistics. One way of solving this is by adding such clusters together, to obtain sufficiently large numbers. This is done by Pooley & Hut (2006). In this process, the information on the indicidual clusters is lost.

To avoid this problem, we fit as follows. The probability of observing $N$ when $\mu$ is expected according to a Poisson distribution is

$$P(N,\mu) = \frac{\mu^N}{N!}e^{-\mu} \tag{4.1}$$

An important aspect of the Poison function for our application is its asymmetry: $P(3, 0.1) \ll P(0, 3)$, i.e. the probability of observing 3 sources when 0.1 is expected is very much smaller than the probability of observing 0 sources when 3 are expected. We now consider

$$N_h = N_c + N_b = \mu_c + \mu_b \qquad \text{with} \qquad \mu_c \equiv a\Gamma + bM \tag{4.2}$$

Both $N_c$,$N_b$ are realizations of Poisson distributions given by $\mu_c$ and $\mu_b$ respectively. $\mu_b$ is determined for each cluster separately, e.g. from the observed number of sources well outside the half-mass radius. For each value of $N_c$ we take $N_b = N_h - N_c$, and then compute the combined probability $P(N_c, \mu_c)P(N_b, \mu_b)$. We then select the $N_c$,$N_b$ pair with the highest combined probability (Fig. 5). The fitting procedure consists of varying $a$ and $b$ to maximize

$$P = \prod_j [P(N_c, \mu_c)P(N_b, \mu_b)]_j \tag{4.3}$$

where $j$ indexes the clusters.

Table 1 lists the numbers that we use in our fitting. We note from the Table that mass cannot be used as a proxy for collision number. The cluster with the highest collision number has a ratio $\Gamma/M \simeq 7$ (normalized on M 4), the cluster with the highest mass has $\Gamma/M \simeq 0.2$. This suggests that mass and collision number can be well discriminated, and we confirm this below. The derived values for $N_h$ and $\mu_b$ (for sources with $L_{0.5-6.0\mathrm{keV}} > 4 \times 10^{30}$ erg/s) correlate with the derived values of $\Gamma$ and $M$, since all are based on

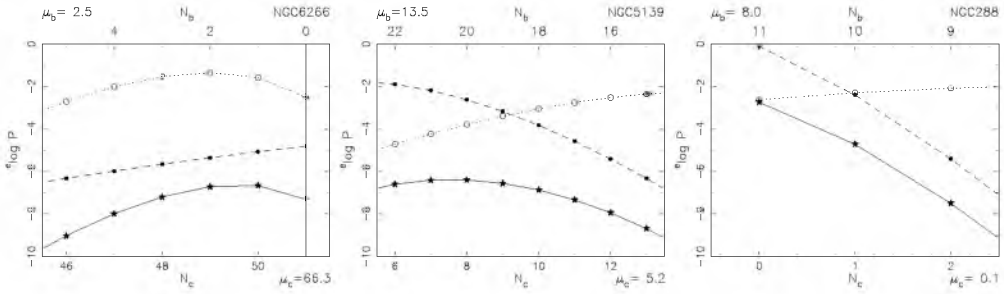


**Figure 5.** Three examples of the combined fit of the number of cluster sources $N_c$ and background sources $N_b$ for one cluster. The expected number of cluster sources $\mu_c$ according to the model $N_c = 1.5\Gamma$, and the expected number of background sources $\mu_b$ are indicated with each frame. For each realization $N_c \leqslant N_h$ the accompanying realization is $N_b \equiv N_h - N_c$. E.g. in NGC 6266 the observed number $N_h = 51$, allowing the combined realizations of $N_c, N_b$ as 51,0 or 50,1 or 49,2 etc. The probability $P(N_c, \mu_c)$ is indicated with a dashed line; the probability $P(N_b, \mu_b)$ with a dotted line; and the combined probability – the product of these for each allowed pair – with a solid line. The cases shown are from left to right for low, roughly equal, and dominant background ($\mu_b \ll N_h$, $\mu_b \sim 0.5N_h$, $\mu_b \gg \mu_c$).

| cluster | $\Gamma$ | $M$ | $N_h$ | $\mu_b$ | $N_s$ |
|---|---|---|---|---|---|
| NGC 6266 | 44.2 | 6.3 | 51 | 2.5 | |
| NGC 104 | 29.7 | 7.7 | 45 | 4.0 | |
| NGC 6626 | 12.6 | 2.5 | 26 | 2.5 | |
| NGC 6752 | 6.0 | 1.6 | 11 | 2.5 | |
| NGC 7099 | 4.7 | 1.2 | 7 | 1.5 | |
| NGC 5904 | 4.1 | 4.4 | 16 | 5.5 | |
| NGC 5139 | 3.5 | 17.2 | 28 | 13.5 | |
| NGC 6397 | 2.4 | 0.6 | 12 | 0.5 | |
| NGC 6121 | ≡1.0 | ≡1.0 | 5 | 2.0 | |
| NGC 6809 | 0.2 | 1.4 | 15 | 7.0 | 3 |
| NGC 6366 | 0.1 | 0.3 | 5 | 4.0 | 1 |
| NGC 288 | 0.0 | 0.7 | 11 | 8.0 | 2 |

**Table 1.** Collision number $\Gamma$ and mass $M$, normalized on the values for NGC 6121, for clusters studied with Chandra, together with the number $N_h$ of sources within the half-mass radius, the expected contribution of background sources $\mu_b$, and the number of secure members $N_s$. Most values $N_h$ and $\mu_b$ are from Pooley et al. (2003); those for NGC 288, NGC 6366 and NGC 6809 are from estimated conversion of $L_{0.5-2.5\,\mathrm{keV}}$ as given in Kong et al. (2006) and Bassa et al. (2007) to $L_{0.5-6.0\,\mathrm{keV}}$. Collision numbers and masses are derived from the central density (in $L_\odot\,\mathrm{pc}^{-3}$), core radii, and absolute magnitudes given in the Feb 2003 version of the Harris (1996) compilation, and they are scaled on the values for M 4 = NGC 6121. Thus we assume that the mass to light ratio is the same for all clusters.

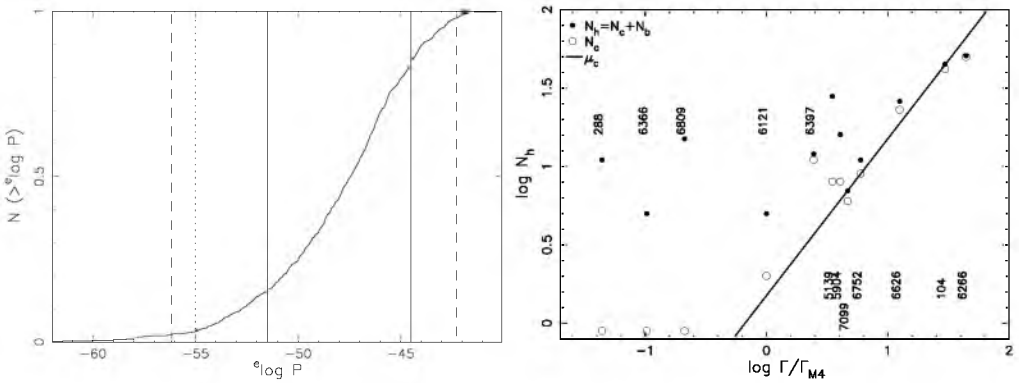


**Figure 6.** Left: distribution of $^e\log P$ for 1000 random realizations of the best model $\mu_c = 1.5\Gamma$, with the 1- and 2-$\sigma$ ranges indicates by solid and dashed lines. The $^e\log P$ value for the best fit is indicated with a dotted line. Right: The best model for $\mu_c = 1.5\Gamma$ is indicated with a solid line, the best number $N_c$ with $\circ$ ($< 0$ indicates $N_c = 0$), and the observed number $N_h = N_c + N_b$ with $\bullet$.

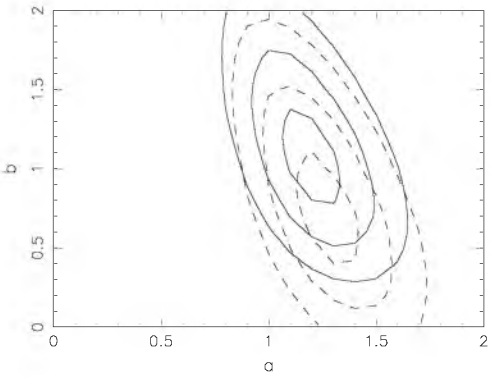


**Figure 7.** 1,2,3-$\sigma$ contours for the best values for the model of Eq. 4.2. Dashed contours are for the fits which allow all observed sources to be background sources, solid contours for the fits where a minimum of secure cluster sources is imposed.

assumed values for the cluster distance $d$ and interstellar absorption $A_V$. For the clusters in the Table the correlations thus introduced are small compared to the ranges of $\Gamma$ and $M$, because the cluster distances are relatively well known, and we ignore them in what follows.

The models we fit all have the form given by Eq. 4.2. We first fit models with $b = 0$, i.e. assuming that the number of cluster sources depends only on the collision number. The best solution has $a = 1.5$ and is shown in Figure 6. The total probability as defined in Eq. 4.3 is $P = e^{-55}$. To see whether this is acceptable, we have used a random generator to produce 1000 realizations by drawing random numbers from Poisson distributions with values $\mu_c$ as given by the best model and $\mu_b$ as listed in Table 1, and for each realization computed the total probability $P$. The cumulative distribution of $^e\log P$ is also shown in Figure 6: the best solution is within the 95% range around the median value, and thus acceptable.

Our next fit allows non-zero values for $a$ and $b$, i.e. allows a linear dependence both on mass and on collision number. The best solution now has $a = 1.3$ and $b = 0.7$; contours of 1,2,3 $\sigma$ around these best values are shown in Figure 7, where we assume that the distribution of $-2(^e\log P - ^e \log P_{\max})$ is given by a $\chi^2$ statistic with one degree of freedom. ($P_{\max}$ is the total probability of the best solution.) We see that the solution with $b = 0$ is marginally acceptable, i.e. the evidence for the mass dependence is marginal. Because we find an acceptable solution for $\Gamma$ as given by Eq. 3.2, there is no need for a different dependence on central density.

Our final fit uses more information, *viz.* the number of (almost) certain cluster members among the X-ray sources, as determined though optical identifications. The importance of this may be seen from Fig. 5 for NGC 288. With an estimated background $\mu_b = 8$ and, for a model depending on collision number only, $\mu_c \simeq 0.1$, the most probable solution is that all 11 sources within the half-mass radius are background sources (cf. Fig. 6). If we add the constraint that at least two sources included in $N_h$ are cluster members (Kong et al. 2006) this solution is no longer possible, and the post probable solution now has $N_c = 2$ and $N_b = 9$. Because the collision number is so small, any cluster source must be a primordial binary, as indeed argued by Kong et al. The best solution for all clusters combined now has $a = 1.2$ and $b = 1.1$, and the solution with $b = 0$ now lies well outside the 3-$\sigma$ contour, i.e. the dependence on mass $M$ is significant (Fig. 7).

## 5. Conclusions

- mass $M$ is *not* a proxy for collision number $\Gamma$
- the number of dim sources scales both with collision number $\Gamma$ and with mass $M$

- scaling with mass only is not acceptable
- correct treatment of the background is important, esp. for faint sources
- to prove the mass-dependence optical identifications are essential

## References

Bassa, C., Pooley, D., Homer, L., & et al. 2004, ApJ, 609, 755
Bassa, C., Pooley, D., Verbunt, F., & et al. 2007, A&A, to be submitted
Becker, W., Swartz, D., Pavlov, G., & et al. 2003, ApJ, 594, 798
Davies, M. 1997, MNRAS, 288, 117
Dempsey, R., Linsky, J., Fleming, T., & Schmitt, J. 1993, ApJS, 86, 599
Edmonds, P., Gilliland, R., Heinke, C., & Grindlay, J. 2003, ApJ, 596, 1177
Ferraro, F., Possenti, A., D'Amico, N., & Sabbi, E. 2001, ApJ, 561, L93
Grindlay, J., Heinke, C., Edmonds, P., & Murray, S. 2001, Science, 292, 2290
Harris, W. 1996, AJ, 112, 1487
Heggie, D. 1981, Megalithic Science, Ancient Mathemathics and Astronomy in Northwest Europe (London: Thames and Hudson)
Heinke, C., Edmonds, P., Grindlay, J., & et al. 2003, ApJ, 590, 809
Heinke, C., Grindlay, J., Edmonds, P., & et al. 2005, ApJ, 625, 796
Hünsch, M., Schmitt, J., Sterzik, M., & Voges, W. 1999, A&AS, 135, 319
Ivanova, N., Heinke, C., Rasio, F., & et al. 2006, MNRAS, 372, 1043
Kong, A., Bassa, C., Pooley, D., & et al. 2006, ApJ, 647, 1065
Maxted, P., Marsh, T., & Moran, C. 2002, MNRAS, 332, 745
McCluskey, S. 1998, Astronomies and cultures in early medieval Europe (C.U.P.)
Ponman, T., Belloni, T., Duck, S., & et al. 1995, MNRAS, 276, 495
Pooley, D. & Hut, P. 2006, ApJ, 646, L143
Pooley, D., Lewin, W., Anderson, S., & et al. 2003, ApJ, 591, L131
Pooley, D., Lewin, W., Homer, L., & et al. 2002a, ApJ, 569, 405
Pooley, D., Lewin, W., Verbunt, F., & et al. 2002b, ApJ, 573, 184
Ruggles, C. 1999, Astronomy in prehistoric Britain and Ireland (New Haven: Yale Univ. Press)
van der Sluys, M., Verbunt, F., & Pols, O. 2006, A&A, 460, 209
Verbunt, F. 2001, A&A, 368, 137
Verbunt, F., Bunk, W., Ritter, H., & Pfeffermann, E. 1997, A&A, 327, 602
Verbunt, F. & Hut, P. 1987, in The Origin and Evolution of Neutron Stars, IAU Symposium No. 125, ed. D. Helfand & J.-H. Huang (Dordrecht: Reidel), 187–197
Verbunt, F. & Lewin, W. 2006, in Compact stellar X-ray sources, ed. W. Lewin & M. van der Klis (Cambridge University Press), 341–379
Verbunt, F., Wheatley, P., & Mattei, J. 1999, A&A, 346, 146
Webb, N., Wheatley, P., & Barret, D. 2006, A&A, 445, 155
Webbink, R. 1984, ApJ, 277, 355
Wijnands, R., Heinke, C., & Grindlay, J. 2002, ApJ, 572, 1002